NJC

Cite this: *New J. Chem.*, 2012, **36**, 1180–1186

www.rsc.org/njc

PAPER

Syntheses, crystal structures and magnetic properties of two low-dimensional cyano-bridged Cr^{III}–$Mn^{II/III}$ assemblies†

Xiaoping Shen,*[a] Qian Zhang,[a] Hongbo Zhou,[a] Hu Zhou[b] and Aihua Yuan[b]

Received (in Montpellier, France) 18th November 2011, Accepted 16th February 2012
DOI: 10.1039/c2nj20966g

Two low-dimensional cyano-bridged Cr^{III}–$Mn^{II/III}$ assemblies $\{[Mn(salpn)][Cr(CN)_6]\}_n \cdot 2n[Mn(salpn)(CH_3OH)_2] \cdot 2nH_2O$ (**1**) (salpn = *N*,*N*′-1,2-propylenebis(salicylideneiminato)dianion) and $\{[Mn(bipy)_2]_2(H_2O)Cl\}[Cr(CN)_6] \cdot 2H_2O$ (**2**) (bipy = 2,2′-bipyridine) have been synthesized and characterized by thermal analyses, single crystal X-ray structural analyses and magnetic measurements. Complex **1** consists of $[(CN)_5Cr^{III}–CN–Mn^{III}(salpn)]_n^{2n-}$ anionic chains, isolated $[Mn^{III}(salpn)(CH_3OH)_2]^+$ cations, and crystallized water molecules. Each $[Cr(CN)_6]^{3-}$ unit connects two adjacent $[Mn^{III}(salpn)]^+$ moieties through *trans*-cyano groups, resulting in the formation of an anionic one-dimensional (1-D) wave-like chain. Complex **2** is composed of trinuclear clusters of $\{[Mn(bipy)_2]_2(H_2O)Cl\}[Cr(CN)_6]$ and guest water molecules. In the trinuclear entity, the $[Cr(CN)_6]^{3-}$ unit connects two neighboring $[Mn^{II}(bipy)_2(H_2O)_{0.5}Cl_{0.5}]^{1.5+}$ moieties in a *trans* fashion through two cyano ligands. Magnetic studies reveal that complexe **1** behaves as a ferrimagnet with critical temperature T_c of 4.5 K resulted from the interchain magnetic interactions, while complex **2** exhibits intramolecular antiferromagnetic coupling.

Introduction

During the past decades, there has been intense interest in the molecule-based magnets of cyano-bridged heterometallic assemblies because of their excellent properties and intriguing architectures.[1–4] It has been found that hexacyanochromate $[Cr(CN)_6]^{3-}$, as a carrier of three unpaired electrons, is an excellent building block for constructing high-T_c magnets with multi-dimensional (2-D and 3-D) structures.[5–8] In contrast, the low-dimensional (polynuclear and 1-D) magnetic assemblies derived from the $[Cr(CN)_6]^{3-}$ building block are relatively rare.[9,10] Nowadays, single molecule magnets (SMMs) and single chain magnets (SCMs) (also referred to as magnetic nanowires) are two hot topics in the field of molecule-based magnetic materials[3,10–12] and as a result, much attention has been paid to the design and construction of low-dimensional cyano-bridged complexes.[13] In our previous work, an interesting heptanuclear assembly $[Cr\{(CN)Mn(salen \cdot H_2O)\}_6][Cr(CN)_6] \cdot 6H_2O$[14] was reported using $[Cr(CN)_6]^{3-}$ and the Mn(III)-Schiff base complex $[Mn^{III}(salen)]^+$ [salen = *N*,*N*′-ethylenebis(salicylideneiminato)dianion] as building blocks. It is well known that the accessorial ligands have a great influence on the structures and magnetic properties of cyano-bridged bimetallic assemblies. To explore the influence of the Schiff base ligand on the resulting assemblies and magnetic properties, we used another Mn(III)-Schiff base complex $[Mn^{III}(salpn)]^+$ [salpn = *N*,*N*′-1,2-propylenebis(salicylideneiminato)dianion] instead of $[Mn^{III}(salen)]^+$ as the building block to react with the $[Cr(CN)_6]^{3-}$ precursor, forming a new 1-D cyano-bridged assembly $\{[Mn^{III}(salpn)][Cr(CN)_6]\}_n \cdot 2n[Mn(salpn)(CH_3OH)_2] \cdot 2nH_2O$ (**1**). In addition, in order to explore the influence of the oxidation state of metal ions on constructing new magnetic materials, the $[Cr(CN)_6]^{3-}$-based trinuclear complex of $\{[Mn^{II}(bipy)_2]_2(H_2O)Cl\}[Cr(CN)_6] \cdot 2H_2O$ (**2**) (bipy = 2,2′-bipyridine) with isotropic Mn^{II} ions was also synthesized using $[Mn^{II}(bipy)_2]^{2+}$ as the building block.

Herein, we report the synthesis, crystal structures and magnetic properties of the two complexes. Magnetic investigation reveals that complex **1** behaves as a ferrimagnet with critical temperature T_c of 4.5 K resulted from the interchain magnetic interactions, while complex **2** exhibits intramolecular antiferromagnetic coupling through cyano-bridges.

Experimental

Materials

All chemicals and solvents were reagent grade and were used without further purification. The complexes $K_3[Cr(CN)_6]$,[15] $[Mn^{III}(salpn)]ClO_4 \cdot 2H_2O$[16] and $Mn^{II}(bipy)_2Cl_2$[17] were prepared by following previously reported procedures.

Caution: Cyanides are highly toxic and should be handled with great caution. We worked at the mmol scale and all the

[a] *School of Chemistry and Chemical Engineering, Jiangsu University, Zhenjiang 212013, China. E-mail: xiaopingshen@163.com; Fax: +86 511-88791800; Tel: +86 511-88791800*
[b] *School of Material Science and Engineering, Jiangsu University of Science and Technology, Zhenjiang 212003, China*

† Electronic supplementary information (ESI) available: Tables S1–S3 and Fig S1. CCDC reference numbers 853097 (**1**) and 853098 (**2**). For ESI and crystallographic data in CIF or other electronic format see DOI: 10.1039/c2nj20966g

Table 1 Summary of the crystallographic data and refinement details for **1** and **2**

	1	**2**
Formula	$C_{61}H_{68}CrMn_3N_{12}O_{12}$	$C_{46}H_{42}ClCrMn_2N_{14}O_5$
Formula weight	1378.09	1068.27
Crystal system	Triclinic	Orthorhombic
Space group	$P\bar{1}$	*Pnn*2
a/Å	10.4784(14)	10.1986(12)
b/Å	17.878(2)	18.9137(13)
c/Å	18.9670(18)	13.8337(19)
α/°	71.198(1)	90
β/°	87.749(3)	90
γ/°	76.002(2)	90
V/Å^3	3260.8(6)	2668.4(5)
Z	2	2
D_c/g cm^{-3}	1.404	1.330
μ(Mo-K*α*)/mm^{-1}	0.798	0.771
F(000)	1426	1094
θ Range/°	1.1–25.5	2.2–26.0
Reflections collected	25 060	19 263
Independent reflections (R_{int})	11 889(0.031)	5254(0.066)
Reflections observed [$I > 2\sigma(I)$]	8303	4031
Parameters refined	824	326
S	1.09	1.05
R_1[a][$I > 2\sigma(I)$] (all)	0.0534(0.0818)	0.0545(0.0737)
wR_2[b][$I > 2\sigma(I)$] (all)	0.0998(0.1043)	0.1137(0.1225)
Flack *x*		0.01(3)

[a] $R_1 = \sum(|F_o| - |F_c|)/\sum|F_o|$. [b] $wR_2 = \{\sum[w(F_o^2 - F_c^2)^2]/\sum[w(F_o^2)^2]\}^{1/2}$ and $w = 1/[\sigma^2(F_o^2) + (aP)^2 + bP]$ with $P = [F_o^2 + 2F_c^2]/3$, $a = 0.0438$ (**1**) and 0.05 (**2**), and $b = 0$ (**1**) and 1.99 (**2**).

preparations were performed in a well ventilated hood. Concentrated aqueous solutions of sodium hypochlorite and sodium hydroxide were used to transform the cyanide from waste into cyanate.

Preparations

{[Mn(salpn)][Cr(CN)$_6$]}$_n$·2*n*[Mn(salpn)(CH$_3$OH)$_2$]·2*n*H$_2$O (1). A methanol solution (10 mL) of [Mn^{III}(salpn)]ClO$_4$·2H$_2$O (0.1 mmol) was added to an aqueous solution (10 mL) of K$_3$[Cr(CN)$_6$] (0.1 mmol). The resulting solution was filtered and the filtrate was left to allow slow evaporation in the dark at room temperature. Black block crystals of complex **1** were obtained after two weeks, washed with MeOH and H$_2$O, respectively, and dried in air. Yield: 60%. Anal. found: C, 53.30; H, 4.83; N, 12.38; Cr, 3.67; Mn, 11.85%. Calcd for $C_{61}H_{68}CrMn_3N_{12}O_{12}$: C, 53.16; H, 4.97; N, 12.20; Cr, 3.77; Mn, 11.96%. IR: $\nu_{C\equiv N}$: 2130 cm^{-1}.

{[Mn(bipy)$_2$]$_2$(H$_2$O)Cl}[Cr(CN)$_6$]·2H$_2$O (2). Greenish yellow crystals of this complex were obtained by slow diffusion of an aqueous solution (10 mL) of K$_3$[Cr(CN)$_6$] (0.1 mmol) and an aqueous solution (10 mL) of Mn^{II}(bipy)$_2$Cl$_2$ (0.1 mmol) through an H-tube at room temperature. The resulting crystals were collected, washed with H$_2$O, and dried in air. Yield: 65%. Anal. found: C, 53.45; H, 3.78; N, 18.96; Cr, 5.10; Mn, 10.59%. Calcd for $C_{46}H_{38}ClCrMn_2N_{14}O_3$: C, 51.72; H, 3.96; N, 18.36; Cr, 4.87; Mn, 10.29%. The existence of Cl was confirmed by energy-dispersive X-ray spectrometry with the molar ratio of Cl : Cr : Mn close to 1 : 1 : 2. IR: $\nu_{C\equiv N}$: 2138, 2133 and 2119 cm^{-1}.

Physical measurements

Elemental analyses for C, H and N were performed on a Perkin-Elmer 240 C microanalysis instrument. Mn and Cr analyses were made on a Jarrell-Ash 1100 + 2000 inductively coupled plasma quantometer. The Cl element was examined by an energy-dispersive X-ray spectrometer. IR spectra were recorded on a Nicolet FT-170SX spectrometer with KBr pellets in the 4000–400 cm^{-1} region. The thermoanalysis was carried out with a NETZSCH STA449C thermal analyzer, which allows simultaneous thermogravimetry (TG) and differential scanning calorimetry (DSC) measurements. The magnetic measurements were performed using a Quantum Design MPMS-XL SQUID magnetometer. Diamagnetic corrections were made using Pascal's constants.[18]

X-Ray crystallography

Diffraction data for **1** and **2** were collected on a Bruker Smart APEX diffractometer equipped with Mo Kα ($\lambda = 0.71073$ Å) radiation. Diffraction data analysis and reduction were performed with SMART, SAINT, and XPREP.[19] Correction for Lorentz, polarization, and absorption effects was performed with SADABS.[20] Structures were solved using a direct method with SHELXS-97 and refined using SHELXL-97.[21] All non-hydrogen atoms were refined with anisotropic thermal parameters. The H atoms of chelated ligands (salpn and bipy), and coordinated methanol molecules were calculated at idealized positions and included in the refinement in a riding mode with U_{iso} for H assigned as 1.2 (or 1.5) times U_{eq} of the attached atoms. The H atoms of coordinated and crystallized water molecules were located from difference maps and refined as riding (O–H = 0.85 Å), with U_{iso}(H) = 1.2U_{eq}(O). In the structure of complex **2**, the site coordinated to the Mn1 atom was split into two positions (Cl1 and O1), with 50% site occupancy each. In addition, one of the crystallized water molecules in complex **2** is disordered in two positions, each site being given an occupancy factor of 0.5. The crystallographic data and experimental details for structural

analyses are summarized in Table 1. Selected bond lengths and angles are listed in Tables S1–S3 in ESI.†

Results and discussion

Thermal analysis

Thermoanalyses for complexes **1** and **2** (Fig. S1 in ESI†) were carried out under a nitrogen atmosphere with a heating rate of 10 °C min^{-1}. With increasing temperature, complex **1** shows a well-pronounced weight loss of 13.51% in the temperature range of 21–107 °C, which can be attributed to the loss of two guest water molecules and coordinated methanol molecules (calcd. 11.70%). The slightly larger weight loss value is probably owing to the adsorbed water in the sample before the measurement. After that, the intermediate product remains stable until 243 °C. At temperatures above 243 °C, the framework decomposition occurs. The thermal behaviour of complex **2** is similar to **1**. The weight loss of 8.35% at the initial stage is consistent with the loss of one coordinated and four crystallized water molecules (calcd. 8.4%). The framework remains stable until 218 °C and collapses above this temperature.

Crystal structure

{[Mn(salpn)][Cr(CN)$_6$]}$_n$·2n[Mn(salpn)(CH$_3$OH)$_2$]·2nH$_2$O (1). The molecular structure of complex **1** consists of $[(CN)_5Cr^{III}–CN–Mn^{III}(salpn)]_n^{2n-}$ anionic chains, $[Mn^{III}(salpn)(CH_3OH)_2]^+$ cations and crystallized water molecules (Fig. 1a). In the $[(CN)_5Cr^{III}–CN–Mn^{III}(salpn)]_n^{2n-}$ chain, each $[Cr(CN)_6]^{3-}$ moiety connects two $[Mn^{III}(salpn)]^+$ units with its two *trans*-C≡N groups, while each $[Mn^{III}(salpn)]^+$ unit is linked to two $[Cr(CN)_6]^{3-}$ ions in *trans* positions. $[Cr(CN)_6]^{3-}$ and $[Mn^{III}(salpn)]^+$ alternately linked through the cyanide-bridges, resulting in a wave-like $Cr^{III}–Mn^{III}$ bimetallic anionic chain (Fig. 1b), in which the two independent Cr atoms (Cr1 and Cr2) both lie on inversion centres. The isolated $[Mn^{III}(salpn)(CH_3OH)_2]^+$ cations act as counterions to keep the electrical neutrality of the crystal. In the structure of **1**, the $[Cr(CN)_6]^{3-}$ fragment is coordinated by six cyano groups and exhibits a distorted octahedral geometry, typical of the hexacyanochromate-based complexes.[7–10] The Cr–C–N angles are nearly linear (173.3(3)–177.6(3)° for Cr1 and 175.7(3)–179.5(3)° for Cr2), and the C≡N bond distances are in the range of 1.159(4)–1.165(4) Å for Cr1 and 1.118(5)–1.168(4) Å for Cr2. The three independent Mn(III) centers (Mn1, Mn2 and Mn3) exhibit distorted octahedral coordination geometries, in which the equatorial sites are occupied by nitrogen and oxygen atoms from the ligand salpn with the Mn–N/O bond distances of 1.870(2)–1.994(3) Å, while the axial positions are occupied by two nitrogen atoms from bridging cyano groups with Mn3–N_{ax} distances of 2.312(3) and 2.359(3) Å in the $[(CN)_5Cr^{III}–CN–Mn^{III}(salpn)]_n^{2n-}$ chain, or are occupied by two oxygen atoms from methanol molecules with Mn–O_{ax} distances of 2.316(2) and 2.257(2) Å for Mn1 and 2.305(2) and 2.256(2) Å for Mn2 in the $[Mn^{III}(salpn)(CH_3OH)_2]^+$ anions. The fact that the axial Mn–N(O)$_{ax}$ distances are much longer than those of equatorial ones can be attributed to the Jahn–Teller effects of Mn(III) ions.[9,14,22] In addition, the Mn–N–C(cyano) bond angles are strongly bent (146.5(3)° and 146.7(2)°) in opposition to the case of the almost linear Cr–C–N angles. These metric parameters are reminiscent of those in related complexes containing Mn(III) and Schiff base ligands.[12,14]

In complex **1**, the intrachain Cr–Mn distances through the cyano bridges are *ca.* 5.248 and 5.299 Å, while the nearest interchain Cr–Mn, Cr–Cr, Mn–Mn distances are *ca.* 9.256, 10.478 and 10.478 Å, respectively. The neighboring chains weakly interact with isolated $[Mn(salpn)(CH_3OH)_2]^+$ cations and crystallized water molecules through hydrogen bonding (Table S2, ESI†), leading to the formation of a 2-D supramolecular layer (Fig. 2).

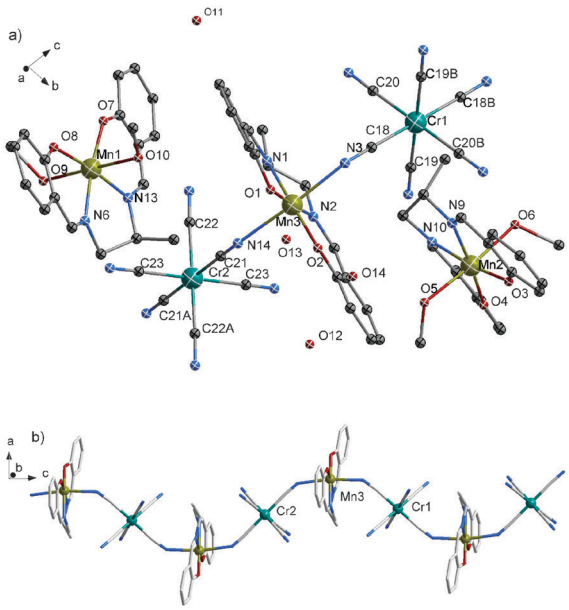

Fig. 1 Molecular view of complex **1** showing (a) ORTEP diagram with 30% thermal ellipsoids and (b) bimetallic chain structure. Symmetry transformations used to generate equivalent atoms: $A = -x, 1-y, -z$; $B = -x, 1-y, 1-z$.

{[Mn(bipy)$_2$]$_2$(H$_2$O)Cl}[Cr(CN)$_6$]·2H$_2$O (2). The molecular structure of complex **2** consists of the heterotrinuclear {[Mn(bipy)$_2$]$_2$(H$_2$O)Cl}[Cr(CN)$_6$] and guest water molecules (Fig. 3). The trinuclear cluster is constituted by a central $[Cr(CN)_6]^{3-}$ mononuclear motif to which two peripheral $[Mn^{II}(bipy)_2(H_2O)_{0.5}Cl_{0.5}]^{1.5+}$ units are connected through two *trans*-C≡N groups. Similar to **1**, the Cr(III) center in the $[Cr(CN)_6]^{3-}$ unit assumes a slightly distorted octahedral coordination geometry. In the $[Mn^{II}(bipy)_2(H_2O)_{0.5}Cl_{0.5}]^{1.5+}$ moiety, the Mn(II) center is six-coordinated by four nitrogen atoms from two 2,2′-bipyridine ligands, one cyano-nitrogen atom, and half oxygen atom as well as half chlorine ion. It is worth noting that one site coordinated to the Mn(II) center is split into two positions (H_2O molecule and counter-ion Cl^-) with 50% site occupancy each due to position disorder. The two 2,2′-bipyridine planes are nearly perpendicular to each other with a dihedral angle of 83.78°. The bond distances of Mn–$N_{(bipy)}$ (2.177(4)–2.290(4) Å) are slightly longer than those of the Mn–$N_{(C\equiv N)}$ (2.113(3) Å). The Mn–Cl bond distance of 2.472(5) Å is close to that found in *cis*-Mn(bipy)$_2$Cl$_2$·EtOH·2H$_2$O (2.483(1) Å).[17] In addition, the Mn–C≡N bond angle is strongly bent (146.6(3)°) as compared with the almost linear

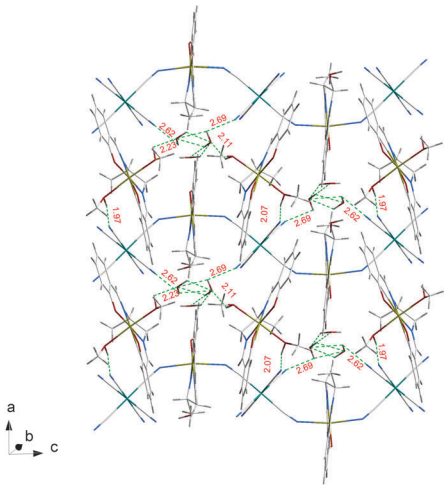

Fig. 2 2-D supramolecular structure of complex **1** induced by interchain hydrogen bonding interactions (the dotted lines show the hydrogen bonds).

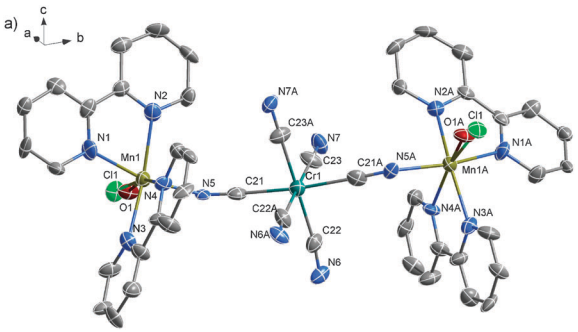

Fig. 3 ORTEP view of complex **2** with 50% thermal ellipsoids, H atoms and the solvent molecules have been omitted for clarity. Symmetry transformations used to generate equivalent atoms: $A = -x, 2 - y, z$.

Cr–C≡N bonds, and the Cr–Mn distances through the cyano bridges are *ca.* 5.159 Å.

Magnetic properties

Magnetic properties of complex 1. The magnetic susceptibilities of complex **1** were measured with an applied field $H = 100$ Oe in the temperature range 1.8–300 K. As shown in Fig. 4, the $\chi_M T$ value per $Mn^{III}_3Cr^{III}$ at 300 K is 11.7 cm^3 K mol^{-1}, which is slightly higher than the spin-only value of 10.9 cm^3 K mol^{-1} expected for an uncoupled spin system (three $S_{Mn} = 2$, one $S_{Cr} = 3/2$) with $g = 2.0$. As the temperature is lowered, the $\chi_M T$ values gradually decrease up to a minimum of 5.8 cm^3 K mol^{-1} at 12 K, and then sharply increase up to a maximum of 89.5 cm^3 K mol^{-1} at 4.5 K. After that, the $\chi_M T$ values again drop rapidly to 34 cm^3 K mol^{-1} at 1.8 K. For the magnetic behavior of complex **1** above 12 K, it is understandable because the CN^- bridge always mediates the antiferromagnetic couplings between Mn(III) and Cr(III).[23] However, the extremely high $\chi_M T$ values at 4.5 K may be the signal of a certain kind of long range magnetic ordering. The decrease of the $\chi_M T$ values below 4.5 K may be due to the zero field split (ZFS) of Mn(III) and/or intermolecular antiferromagnetic interactions. The antiferromagnetic ordering

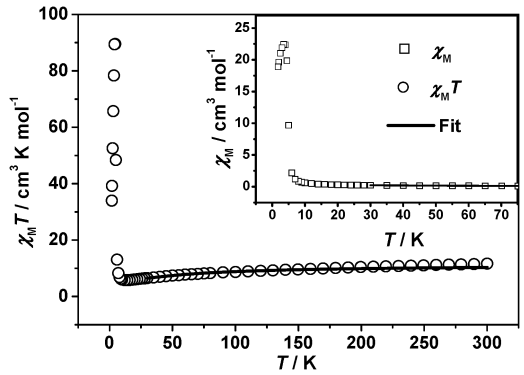

Fig. 4 Temperature dependence of $\chi_M T$ and χ_M (inset) for complex **1** measured at 100 Oe. The solid line is the fitting plot.

can be clearly seen from the plot of χ_M *vs.* T shown in the inset of Fig. 4, in which a peak appears at about 3.5 K. To probe quantitatively the intrachain coupling constant J, an approximate infinite chain model is used to regard the Mn–NC–Cr dimers as the magnetic subunit.[24] The intradimer and interdimer coupling constants are defined as J_d and J_c, respectively. Two mononuclear Mn^{III} moieties are treated as paramagnetic ions. The exchange Hamiltonian is of the form, $H = -J_d S_{Mn} S_{Cr} + g\mu_B H S_{Mn}$ and the magnetic formula is expressed as follows:

$$\chi_d = \frac{Ng^2\mu_B^2}{3kT} \times \frac{3/2 + 30/2e^{3J_d/kT} + 105/2e^{8J_d/kT} + 252/2e^{15J_d/kT}}{2 + 4e^{3J_d/kT} + 6e^{8J_d/kT} + 8e^{15J_d/kT}}$$

$$\chi_d = \frac{Ng^2\mu_B^2}{3kT} S_d(S_d + 1)$$

$$S_d(S_d + 1) = \frac{3}{4} \times \frac{1 + 10e^{3J_d/kT} + 35e^{8J_d/kT} + 84e^{15J_d/kT}}{1 + 2e^{3J_d/kT} + 3e^{8J_d/kT} + 4e^{15J_d/kT}}$$

$$\chi_m = \frac{Ng^2\beta^2}{3kT}\frac{1+u}{1-u} S_d(S_d + 1) + \frac{2Ng^2\mu_B^2}{3kT} S_{Mn}(S_{Mn} + 1)$$

$$u = \coth(J_c S_d(S_d + 1)/kT) - kT/J_c S_d(S_d + 1)$$

where the N, k, T and μ_B have the common meanings, the fitting of experimental χ_M value between 30–300 K gives: $J_d = -2.70$ cm^{-1}, $J_c = -3.60$ cm^{-1}, $g = 2.0$ and $R = 1.3 \times 10^{-4}$. The obtained g value is comparable to those of other Mn^{III} and Cr^{III} systems.[25] The fitting parameters obviously indicate the antiferromagnetic couplings between Mn^{III} and Cr^{III}, which is in agreement with the analyses conducted above and comparable to the fitting results of $[Mn(5\text{-}Clsalmen)(CH_3OH)(H_2O)]_{2n}[\{Mn\text{-}CN\}Cr(CN)_5]_n \cdot 5.5nH_2O$ (**3**) with similar Mn^{III}–Cr^{III} 1-D structure.[26]

The field dependence of the magnetization measured at 1.8 K is shown in Fig. 5. The magnetization increases rapidly at low field, which corresponds to the contribution of the easy magnetized axis of complex **1**. At high field, the magnetization of hard axis operates,[27] and thus it does not fulfill the saturation values of 9 $N\mu_B$ (calculated from $M_S = g(3S_{Mn} - S_{Cr})$ with $g = 2$) until 70 kOe. The tendency of the magnetization increase continues up to 70 kOe for **1**, indicating that the magnetization is still

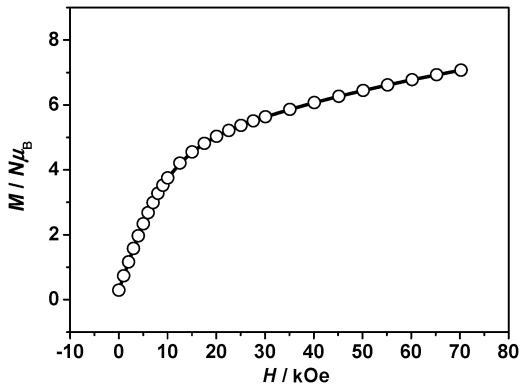

Fig. 5 Field dependence of the magnetization for complex **1** at 1.8 K.

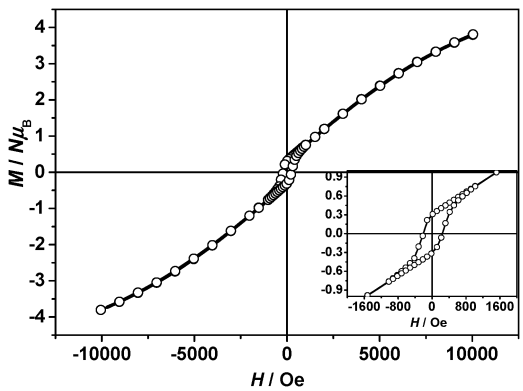

Fig. 6 Magnetic hysteresis loop of complex **1** at 1.8 K. The inset is a magnified view of the low applied field zone.

unsaturated at 70 kOe, which can be ascribed to the magnetic anisotropy as mentioned above.

Furthermore, complex **1** behaves as a ferrimagnet, which is illustrated in Fig. 6. The magnetic hysteresis loop reveals the magnet-like nature of complex **1**. The value of the coercive field is *ca.* 225 Oe. As discussed above, the non-compensation of the spins along the chains orders antiferromagnetically (a peak appearing in the curve of χ_M *vs.* *T*), but the spin canting probably occurs, leading to the spontaneous magnetization. This aspect is quite different from that of the analogue of complex **3**,[26] in which the lack of a maximum in the χ_M *vs.* *T* plot precluded the occurrence of antiferromagnetic ordering.[28] The magnetic phase transition temperature (T_c) of **1** can be determined by alternating current (AC) magnetic measurement, as shown in Fig. 7. AC magnetic susceptibility for **1** at zero direct current (DC) and 3 Oe AC magnetic field shows a frequency-dependent maximum in χ'_M accompanied by χ''_M at about 4.5 K, indicating that T_c of complex **1** is 4.5 K. The slight frequency-dependence of the out of phase component indicates the possible spin glass behavior, which may be related to some disorder in the crystal lattice.[29] However, possible single-chain-magnet behavior cannot be excluded because of the 1-D nature of complex **1**, especially when Mn(III)-Schiff base with significant uniaxial magnetic anisotropy is incorporated into the 1-D system.[12] Though the energy gap to create a domain wall cannot be evaluated quantitatively in the present case, the structural feature and the magnetic behavior suggest strongly that complex **1** shows long range ordering with a slow relaxation process possibly induced

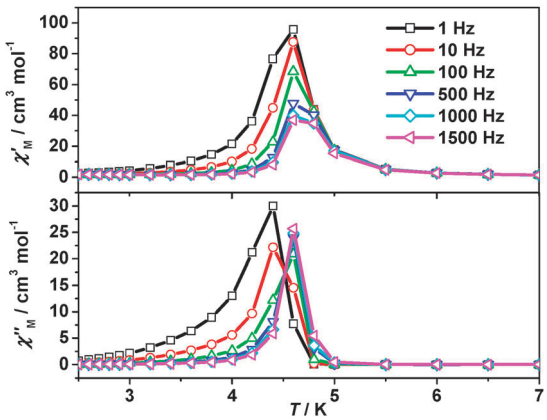

Fig. 7 The real (χ'_M) and imaginary (χ''_M) parts of AC magnetic susceptibility for **1** under 0 DC and 3 Oe AC magnetic field.

by the 1-D magnetic anisotropic chains.[12b,c] Interestingly, despite the difference in magnetic behavior, complexes **1** and **3**[26] are both characterized as ferrimagnets due to their similar structural frameworks. However, the much higher maximum of $\chi_M T$ in **1** (89.5 cm^3 K) than that in **3** (21.71 cm^3 K)[26] implies the stronger long range ordering in **1**. Indeed, the T_c of **1** (4.5 K) is higher than that of **3** (3.0 K).[26] Therefore, the ligands play a crucial role in constructing molecule magnets. In fact, the organic ligands used often not only affect greatly the structure of the resulting magnetic assemblies, but also induce a different ligand field effect and intermolecular short contacts, all of these factors will eventually determine the different magnetic behaviors.

Magnetic properties of complex 2

The magnetic susceptibilities of complex **2** (measured at H = 2 kOe, 1.8–300 K) are shown in Fig. 8. At 300 K, the $\chi_M T$ value per $Mn^{II}_2Cr^{III}$ unit is 9.3 cm^3 K mol^{-1}, which is slightly smaller than the theoretical value of 10.6 cm^3 K mol^{-1} expected for an uncoupled spin system (two S_{Mn} = 5/2, one S_{Cr}, = 3/2) with g = 2.0. Upon lowering the temperature, the $\chi_M T$ values gradually decrease and reach a minimum of 6.9 cm^3 K mol^{-1} at 45 K. Then the values sharply increase up to a maximum of 14.8 cm^3 K mol^{-1} at 4 K. Below 4 K, the $\chi_M T$ values rapidly drop to 11.7 cm^3 K mol^{-1} at 1.8 K. The Curie–Weiss fitting between 80–300 K gives a negative

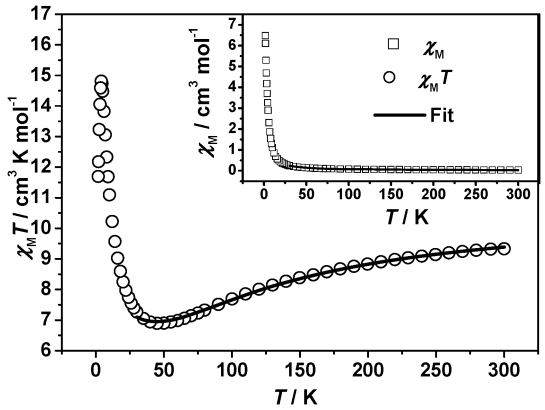

Fig. 8 Temperature dependence of $\chi_M T$ and χ_M (inset) for complex **2** measured at 2 kOe. The solid line is the fitting plot.

Weiss constant $\theta = -34$ K, which reveals the antiferromagnetic coupling between Mn^{II}($S = 5/2$) and Cr^{III}($S = 3/2$). The slight inconsistency between the room-temperature $\chi_M T$ value and the uncoupling theoretical value should be due to the antiferromagnetic coupling effect. The rapid increase of the $\chi_M T$ values reveals the non-compensation of the spins of the trinuclear clusters. It is worth noting that the maximum of 14.8 cm^3 K mol^{-1} is much larger than the spin-only value of 7.8 cm^3 K mol^{-1} expected for an $S = 7/2$ ground state, suggesting the possible presence of magnetic ordering. For the $Mn^{II}_2Cr^{III}$ trinuclear magnetic unit, Kambe's method[30] based on an exchange Hamiltonian of the form $H = -2JS_{Cr}(S_{Mn(1)} + S_{Mn(2)})$ was used for the fitting of experimental $\chi_M T$ values between 30–300 K.

$$\chi_M = \frac{Ng^2\mu_B^2}{4kT} \times \frac{A}{B}$$

$$A = 286 + 165e^{11x} + 84e^{20x} + 35e^{27x} + 165e^{3x} + 84e^{12x} + 35e^{19x} + 10e^{24x} + 84e^{6x} + 35e^{13x} + 10e^{18x} + e^{21x} + 35e^{9x} + 10e^{14x} + e^{17x} + 10e^{12x} + 84e^{30x} + 165e^{21x} + 286e^{10x} + 455e^{-3x}$$

$$B = 6 + 5e^{11x} + 4e^{20x} + 3e^{27x} + 5e^{3x} + 4e^{12x} + 3e^{19x} + 2e^{24x} + 4e^{6x} + 3e^{13x} + 2e^{18x} + e^{21x} + 3e^{9x} + 2e^{14x} + e^{17x} + 2e^{12x} + 4e^{30x} + 5e^{21x} + 6e^{10x} + 7e^{-3x}$$

where $x = -J/kT$. The best-fitting of complex **2** gave $J = -7.2$ cm^{-1}, $g = 2.01$ and $R = 2.1 \times 10^{-3}$. The fitting result also indicates the antiferromagnetic couplings between Mn^{II} and Cr^{III} mediated by a cyano-bridge. The J value is of the same order of magnitude as the exchange coupling parameters determined for the complex $[(MnL)_2Cr(CN)_6(H_2O)_2]\cdot 1/3[Cr(CN)_6]\cdot 10/3H_2O$ (**4**) (L = 2,13-dimethyl-3,6,9,12,18-pentaazabicyclo[12.3.1]octadeca-1(18),2, 12,14,16-pentaene) with Mn^{II}–Cr^{III} trinuclear cations.[31]

The field dependence of the magnetization of complex **2** at 1.8 K is shown in Fig. 9. The magnetization increases abruptly at low field and then gradually up to a saturation value of 6.6 $N\mu_B$ at *ca.* 40 kOe, which is slightly lower than the expected value of 7.0 $N\mu_B$ for the antiferromagnetic $Mn^{II}_2Cr^{III}$ system ($M_S = g(2S_{Mn}–S_{Cr})$). Reduced magnetization $M/N\mu_B$ *vs.* H/T was also measured at applied fields of 70, 60, 50, 40, 30 and 20 kOe at 1.8–10 K. As plotted in Fig. S2 (ESI†), the isofield

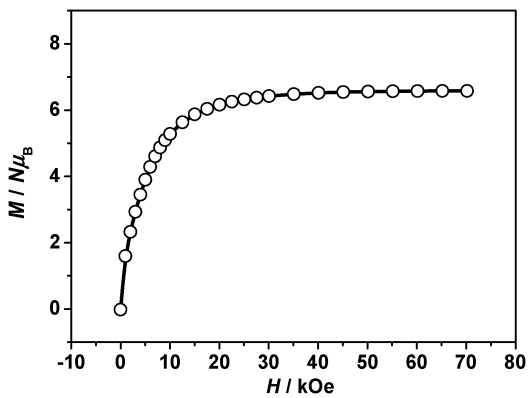

Fig. 9 Field dependence of the magnetization for complex **2** at 1.8 K.

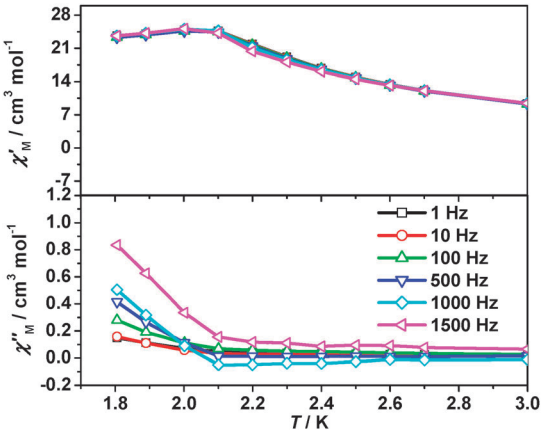

Fig. 10 The real (χ'_M) and imaginary (χ''_M) parts of AC magnetic susceptibility for **2** under 0 DC and 3 Oe AC magnetic field.

lines superimpose, indicating no significant ZFS in complex **2**, which is due to the magnetic isotropy of Cr^{III} and high-spin Mn^{II}.[32] AC magnetic susceptibility of **2** (Fig. 10) shows a frequency-independent maximum in χ'_M accompanied by frequency-dependent χ''_M at about 2.0 K, which indicates the possibility of a certain magnetic phase transition. However, the SMM behavior is not possible because of the lack of negative ZFS parameter (D), as proved by the plot of reduced magnetization $M/N\mu_B$ *vs.* H/T (Fig. S2, ESI†). Consequently, the slightly magnetic slow relaxation phenomenon may be caused by the glassy magnetized state arising from short range ordering through intermolecular interactions, which is comparable to the magnetic behavior of $[(tpm)_2Mn^{II}][W^V_2(CN)_{16}Mn_2(tpm)_2(H_2O)_2]\cdot 4H_2O$.[33]

Conclusion

In this work, we demonstrate how the building block $[Cr(CN)_6]^{3-}$ can be used as precursor towards the preformed $[Mn^{III}(salpn)]^+$ and $[Mn^{II}(bipy)_2]^{2+}$ species to afford cyano-bridged heterometallic 1-D Cr(III)–Mn(III) (**1**) and trinuclear Cr(III)–Mn(II) (**2**) complexes, respectively. The magneto-structural investigation of complex **1** reveals that despite its low-dimensional structure, it shows long range magnetic ordering and behaves as a molecule-based magnet. Interestingly, the slow relaxation of the 1-D chains of complex **1** retains and the relatively strong interchain interactions enhance its critical temperature as compared with the 1-D analogue of **3**.[26] Complex **2** exhibits intramolecular antiferromagnetic coupling. However, a slightly magnetic slow relaxation phenomenon is also observed, which seems to be different from the analogue of **4**.[31] It is worth noting that the structure of complex **1** is completely different from the heptanuclear assembly $[Cr\{(CN)Mn(salen\cdot H_2O)\}_6][Cr(CN)_6]\cdot 6H_2O$ reported by our group previously.[14] Therefore, the accessorial ligands indeed affect not only the structure of cyano-bridged assemblies, but also their magnetic properties, even those with the similar structural skeleton, further indicating the importance of selecting proper secondary ligands for constructing cyano-bridged molecule-based magnets with expected property.

Acknowledgements

The authors are grateful for financial support from the National Natural Science Foundation of China (No. 51072071) and the

Natural Science Foundation of Jiangsu Province (No. BK2009196).

Notes and references

1 M. Verdaguer, A. Bleuzen, V. Marvaud, J. Vaissermann, M. Seuleiman, C. Desplanches, A. Scuiller, C. Train, R. Garde, G. Gelly, C. Lomenech, I. Rosenman, P. Veillet, C. Cartier and F. Villain, *Coord. Chem. Rev.*, 1999, **190–192**, 1023.
2 M. Ohba and H. Ôkawa, *Coord. Chem. Rev.*, 2000, **198**, 313.
3 T. S. Venkatakrishnan, S. Sahoo, N. Brefuel, C. Duhayon, C. Paulsen, A. L. Barra, S. Ramasesha and J. P. Sutter, *J. Am. Chem. Soc.*, 2010, **132**, 6047.
4 C. F. Wang, D. P. Li, X. Chen, X. M. Li, Y. Z. Li, J. L. Zuo and X. Z. You, *Chem. Commun.*, 2009, 6940.
5 T. Mallah, S. Tiebaut, M. Verguer and P. Veillet, *Science*, 1993, **262**, 1554.
6 S. Holmes, M. Girolaml and G. S. Sol-Gel, *J. Am. Chem. Soc.*, 1999, **121**, 5593.
7 M. Ohba, N. Usuki, N. Fukita and H. Ôkawa, *Angew. Chem., Int. Ed.*, 1999, **38**, 1795.
8 H. Z. Kou, S. Gao, J. Zhang, G. H. Wen, G. Su, R. K. Zheng and X. X. Zhang, *J. Am. Chem. Soc.*, 2001, **123**, 11809.
9 H. Miyasaka, H. Takahashi, T. Madanbashi, K. Sugiura, R. Clerac and H. Nojiri, *Inorg. Chem.*, 2005, **44**, 5969.
10 T. Glaser, M. Heidemeier, T. Weyhermüller, R.-D. Hoffmann, H. Rupp and P. Müller, *Angew. Chem., Int. Ed.*, 2006, **45**, 6033.
11 J. J. Sokol, A. G. Hee and J. R. Long, *J. Am. Chem. Soc.*, 2002, **124**, 7656.
12 (*a*) M. Ferbinteanu, H. Miyasaka, W. Wernsdorfer, K. Nakata, K. I. Sugiura, M. Yamashita, C. Coulon and R. Clérac, *J. Am. Chem. Soc.*, 2005, **127**, 3090; (*b*) C. Coulon, R. Clérac, W. Wernsdorfer, T. Colin and H. Miyasaka, *Phys. Rev. Lett.*, 2009, **102**, 167204; (*c*) H. Miyasaka, K. Takayama, A. Saitoh, S. Furukawa, M. Yamashita and R. Clérac, *Chem.–Eur. J.*, 2010, **16**, 3656.
13 R. Lescouëzec, L. Marilena Toma, J. Vaissermann, M. Verdaguer, F. S. Delgado, C. Ruiz-Pérez, F. Lloret and M. Julve, *Coord. Chem. Rev.*, 2005, **249**, 2691.
14 X.-P. Shen, B.-L. Li, J.-Z. Zou and Z. Xu, *Transition Met. Chem.*, 2002, **27**, 372.
15 W. B. Schaap, R. Krishnamurthy, D. K. Wakefield and W. F. Coleman, *Coordination Chemistry*, ed. S. Kirschner, Plenum Press, New York, 1969, p. 177.
16 N. Matsumoto, N. Takemoto, A. Ohyoshi and H. Okawa, *Bull. Chem. Soc. Jpn.*, 1988, **61**, 2984.
17 S. McCann, M. McCann, R. M. T. Casey, M. Jackman, M. Devereux and V. McKee, *Inorg. Chim. Acta*, 1998, **279**, 24.
18 O. Kahn, *Molecular Magnetism*, VCH Publishers, New York, 1993.
19 Bruker, *SMART, SAINT and XPREP: Area Detector Control and Data Integration and Reduction Software*, Bruker Analytical X-ray Instruments Inc., Madison, Wisconsin, USA, 1995.
20 G. M. Sheldrick, *SADABS: Empirical Absorption and Correction Software*, University of Göttingen, Göttingen, Germany, 1996.
21 (*a*) G. M. Sheldrick, *SHELXS-97. Program for X-ray Crystal Structure Determination*, Göttingen University, Göttingen, Germany, 1997; (*b*) G. M. Sheldrick, *SHELXL-97. Program for X-ray Crystal Structure Determination*, Göttingen University, Göttingen, Germany, 1997; (*c*) G. M. Sheldrick, *Acta Crystallogr., Sect. A: Cryst. Phys., Diffr., Theor. Gen. Cryst.*, 2008, **64**, 112.
22 D. Visinescu, L. M. Toma, F. Lloret, O. Fabelo, C. Ruiz-Perez and M. Julve, *Dalton Trans.*, 2009, 37.
23 (*a*) W. R. Entley, C. R. Treadway and G. S. Girolami, *Mol. Cryst. Liq. Cryst.*, 1995, **273**, 153; (*b*) H. Weihe and H. U. Güdel, *Comments Inorg. Chem.*, 2000, **22**, 75; (*c*) S. M. Holmes and G. S. Girolami, *Mol. Cryst. Liq. Cryst.*, 1997, **305**, 279.
24 H. Z. Kou, B. C. Zhou, D. Z. Liao, R. J. Wang and Y. D. Li, *Inorg. Chem.*, 2002, **41**, 6887.
25 (*a*) L. J. Boucher and C. G. Coe, *Inorg. Chem.*, 1975, **14**, 1289; (*b*) B. J. Kennedy and K. S. Murray, *Inorg. Chem.*, 1985, **24**, 1552; (*c*) J. A. Bonadies, M. L. Kirk, M. S. Lah, D. P. Kessissoglou, W. E. Hatfield and V. L. Pecoraro, *Inorg. Chem.*, 1989, **28**, 2037; (*d*) K. Bertoncello, G. D. Fallon, K. S. Murray and R. T. Tiekink, *Inorg. Chem.*, 1991, **30**, 3562; (*e*) S. K. Chandra, P. Chakraborty and A. J. Chakravorty, *J. Chem. Soc., Dalton Trans.*, 1993, 863.
26 C. Yang, Q. L. Wang, J. Qi, Y. Ma, S. P. Yan, G. M. Yang, P. Cheng and D. Z. Liao, *Inorg. Chem.*, 2011, **50**, 4006.
27 H. Miyasaka, H. Ieda, N. Matsumoto, K. Sugiura and M. Yamashita, *Inorg. Chem.*, 2003, **42**, 3509.
28 D. Cangussu, E. Pardo, M.-C. Dul, R. Lescouëzec, P. Herson, Y. Journaux, E. F. Pedroso, C. L. M. Pereira, H. O. Stumpf, M. C. Muñoz, R. Ruiz-García, J. Cano, M. Julve and F. Lloret, *Inorg. Chim. Acta*, 2008, **361**, 3394.
29 H. Z. Kou, B. C. Zhou, S. Gao, D. Z. Liao and R. J. Wang, *Inorg. Chem.*, 2003, **42**, 5604.
30 K. Kambe, *J. Phys. Soc. Jpn.*, 1950, **5**, 48.
31 C. Paraschiv, M. Andruh, Y. Journaux, Z. Žak, N. Kyritsakasd and L. Ricard, *J. Mater. Chem.*, 2006, **16**, 2660.
32 E. Pardo, C. Train, R. Lescouëzec, K. Boubekeur, E. Ruiz, F. Lloret and M. Verdaguer, *Dalton Trans.*, 2010, **39**, 4951.
33 J. Wang, Y. L. Xu, H. B. Zhou, H. S. Wang, X. J. Song, Y. Song and X. Z. You, *Dalton Trans.*, 2010, **39**, 3489.

